

The Exbow MetaSax: Compositional Applications of Bowed String Physical Models Using Instrument Controller Substitution

Matthew Burtner¹ and Stefania Serafin²

¹VCCM, McIntire Department of Music, University of Virginia, Charlottesville, VA, USA and ²CCRMA, Department of Music, Stanford University, Stanford, CA, USA

Abstract

Physical models of musical instruments are interesting from different perspectives. The scientist, being able to reproduce the sound of a particular instrument, shows that the physics of that instrument has been understood. The performer can take advantage of the virtual instruments which are often easier to play than real ones. The composer can use physically modelled instruments to obtain sonorities that cannot be created on the physical instrument. In this paper we explore the boundaries of a physical model by abstracting a bowed string physical model from its analog material controller, and implementing this model within another instrumental controller, the metasaxophone. We focus on different effects that can be obtained through extending the possibilities offered by a physical model of bowed string instruments through the use of alternate controllers.

1. Introduction

Physical models of musical instruments become interesting for composers when sonorities that cannot be achieved with a real instrument can be obtained. In this paper we explore extended techniques for bowed string physical models arising when a traditional instrumental controller is substituted for an entirely different type of controller.

This technique of instrumental controller substitution creates surprising real-time performance possibilities for the physical model, forcing it to function in unconventional ways and generating new timbral possibilities for the composer.

We built a real-time waveguide physical model of a general self-sustained oscillator. The timbral space of the model is controlled using the metasaxophone, a tenor saxophone custom fitted with an on-board computer micro-

processor and an array of sensors used to control live electronics, as described in detail below.

2. A bowed string physical model

We developed a waveguide physical model of a bowed string which is a refinement of the model first proposed by Julius Smith (Smith, 1983).

Fractional delay lines model the generation of transversal and torsional waves on the strings toward the nut and the bridge respectively, and lowpass filters simulate losses at the bridge and nut.

The friction curve is represented by the following equation:

$$\mu = \mu_d + \frac{(\mu_s - \mu_d)v_0}{v_0 + v - v_b} \quad (2.1)$$

where μ_d is the dynamic friction coefficient, μ_s is the static friction coefficient, v_0 is the initial string velocity, v is the current string velocity and v_b is the bow velocity.

Expressing the friction curve using equation 2.1 allows to solve analytically the coupling between the friction curve and the string vibration, i.e., the following system of equation can be solved analytically

$$\begin{cases} f = 2Z(v - v_h) \\ f = f_b \mu \end{cases} \quad (2.2)$$

where Z is the string impedance, v_h is the incoming velocity at the bow point, f_b is the bow force.

As Figure 1 shows, solving the system of equations 2.2 allows to obtain the outgoing velocity v_{on} and v_{ob} propagating toward the nut and the bridge respectively.

Accepted: 8 December, 2001

Correspondence: Dr. Matthew Burtner, VCCM, McIntire Department of Music, University of Virginia, Charlottesville, VA 22903, USA. Tel.: +1 (434) 293-5265, E-mail: mburtner@virginia.edu

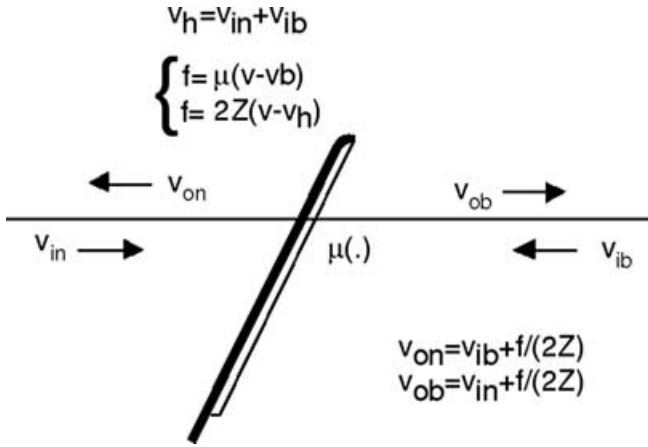


Fig. 1. Equations of a basic bowed string physical model.

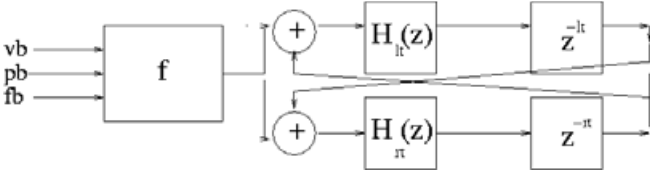


Fig. 2. Block diagram of a basic bowed string physical model.

The block diagram structure of this basic model is shown in Figure 2.

In it f represents the friction curve, while $H_{lt}(z)$ and $H_{rt}(z)$ represent the lowpass filters modeling losses at the fingerboard and the bridge respectively. z^{-lt} and z^{-rt} are the delay lines modeling the wave propagation toward the fingerboard and the bridge respectively.

As Figure 2 shows, the main input parameters driving this model are the bow velocity v_b , the bow pressure f_b , and the bow position p_b .

The model runs in real-time using the Max/MSP platform (Zicarelli, 1998).

To make the model more appealing from a compositional point of view, we extended it as described in the following section.

3. Extending the virtual bowed string

In order to extend the bowed string physical model to create sonorities that cannot be achieved with a real instrument, we first added different kinds of filters in the string loop.

In particular we focused on varying the stiffness of the strings in order to simulate strings of different materials.

Typically in the design of bowed string physical models stiffness is neglected.

However it is well known that stiffness is an important component of other types of vibrating objects such as piano strings or bars.

Specifically, stiffness stretches the frequencies of the partials as follows:

$$\omega_n = n\omega_c \sqrt{1 + Bn^2} \quad (3.1)$$

(Morse, 1981), for $n = 1, 2, \dots$ where $B = (\pi/\kappa L)^2$ is the inharmonicity factor, $\omega_c = \pi c_s/L$ is the fundamental frequency in case of no stiffness, where L is the length of the string.

3.1 Designing allpass filters for dispersion simulation

In order to account for dispersion in the digital waveguide model of the bowed string, we choose a numerical filter made of a delay line $q^{\tau-\tau_0}$, and a n -order stable all-pass filter

$$H(q) = q^{-n} P(q^{-1}) / P(q)$$

where

$$P(q) = p_0 + \dots + p_{n-1}q^{n-1} + q^n,$$

and τ and n are appropriately chosen.

As proposed in (Lang, 1992), we want to minimize the ∞ -norm of a particular frequency weighting of the error between the internal loop phase and its approximation by the filter cascade:

$$\delta_D = \min_{p_1, \dots, p_m} \|W_D(\Omega)[\varphi_d(\Omega) - (\varphi_D(\Omega) + \tau\Omega)]\|_{\infty} \quad (3.2)$$

where $\varphi_D(\Omega)_{\infty}$ is the phase of $H(e^{j\Omega})$, and $W_D(\Omega)$ is the frequency weighting ($W_D(\Omega)$ is zero outside the frequency range, i.e., $[\Omega_c, \Omega_N]$).

From an acoustical point of view, it is important to have a frequency weighting that approximates the way the auditory system perceives the difference between original and simulated phase dispersion.

In order to restrict the approximation to the first few thousand hertz, Rocchesso and Scalcon (Rocchesso & Scalcon, 1996) propose to use frequency warping (Smith & Abel, 1999) together with frequency weighting.

In our implementation, we choose a weighting function that stresses the accuracy at low frequencies, in order to provide a filter design technique that is both correct from a perceptual point of view and interesting from a musical point of view.

3.2 Application to the bowed string model

We inserted the estimated filters in the string loop as shown in Figure 3.

The transversal waves propagating toward the bridge are first filtered by the bridge filters for losses and then by the dispersion filters.

For completeness we inserted in the block diagram also the torsional waves propagation. Torsional waves can be modeled as an additional couple of waveguides whose speed is about 5.2 times the transverse wave speed.

Note how, since the string is a linear system, inverting the three blocks corresponding to the propagation of the waves

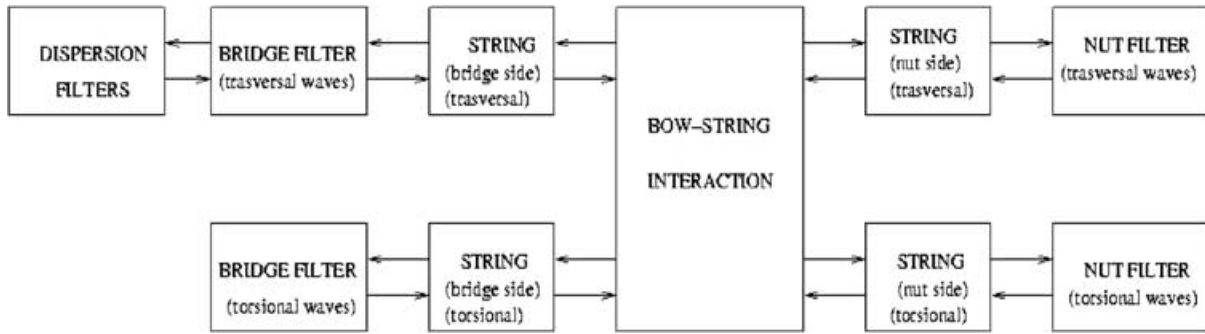


Fig. 3. Block diagram of a bowed string physical model with allpass filters for dispersion simulation.

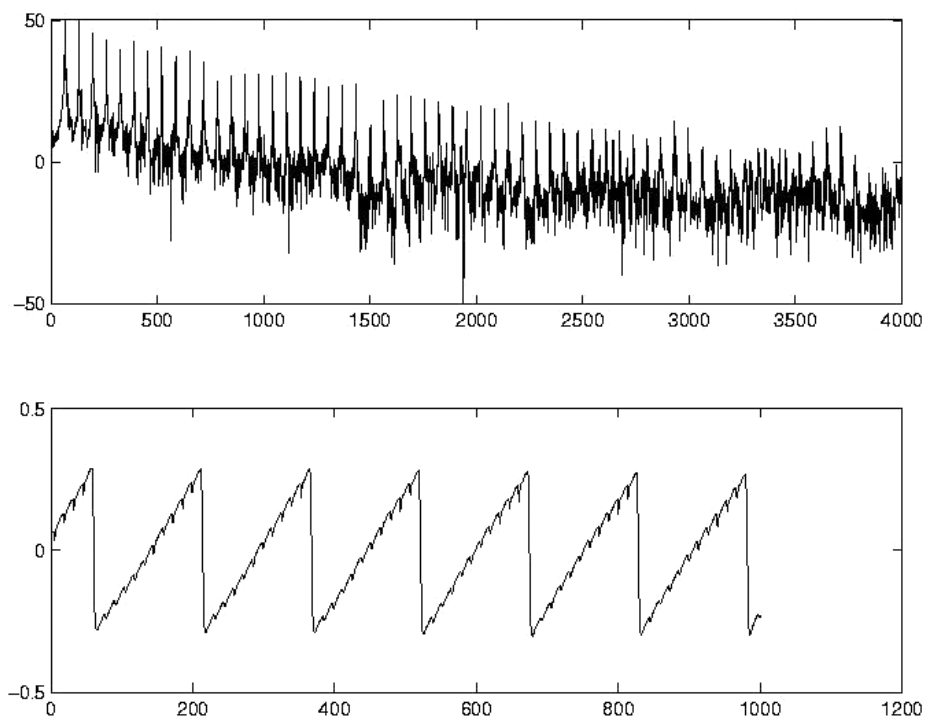


Fig. 4. Bottom: Time domain waveform of a non-stiff string. Top: corresponding spectrum.

in the bridge side of the string would not change the results of the simulation.

3.3 Influence of stiffness in virtual bowed strings

We run our digital waveguide model using a cello *D* string, with bending stiffness $B = 0.0004 \text{ N/m}$.

The string, starting from rest, is excited by a constant bow velocity $v_b = 0.05 \text{ m/s}$, a bow force of $f_b = 0.2 \text{ N}$ and a normalized bow position of 0.08, where 0 represents the bridge while 1 represents the nut.

Figure 5 shows the result of this simulation where the string velocity at the bridge has been captured after a steady state motion is achieved.

The waveform on the bottom of Figures 4 and 5 shows the velocity of a string with no stiffness and stiffness

coefficient $B = 4e - 2 \text{ Nm}^2$, while the waveforms on the top show the corresponding spectrum. Note how the Helmholtz motion gets distorted in the case of the stiff string, which has a significant impact on the quality of the sound synthesis.

3.4 Extending the excitation

In order to further extend the model, we also modified the bow string interaction in two different ways, first modeling a noisy friction model then including different kinds of excitations that do not belong to bowed string models.

First we introduced some noise to the shape of the friction curve. The introduction of noise in friction models was first proposed in (Salisbury et al., 1988).

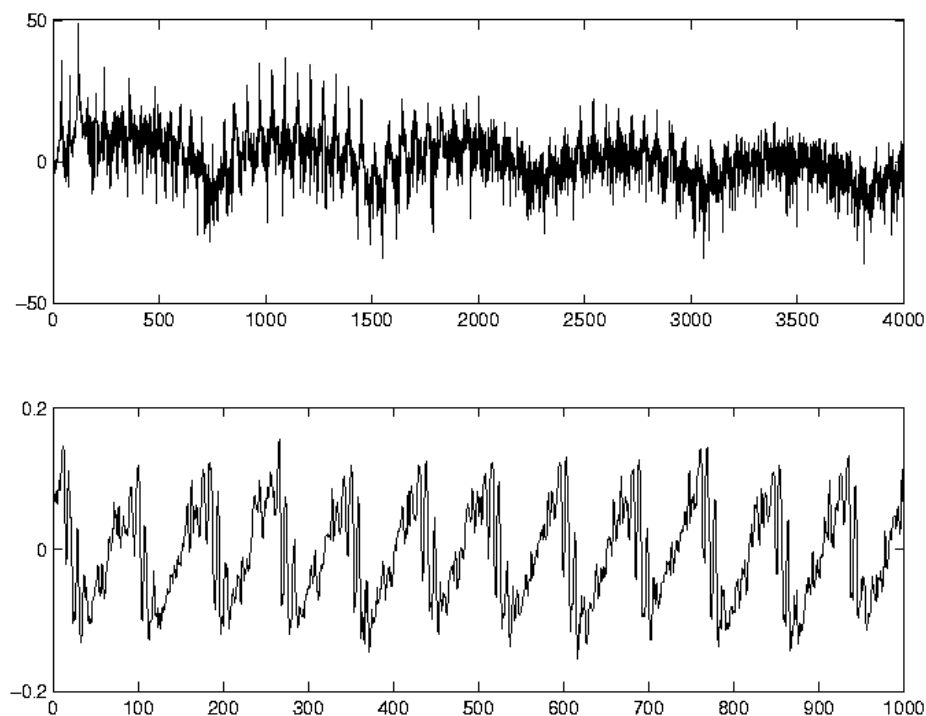


Fig. 5. Bottom: Time domain waveform of a stiff bowed string. Top: Corresponding spectrum.

The level of noise can be increased in real-time and high values completely break the periodicity of the synthetic bowed string oscillation.

We also linearly interpolated the shape of the friction curve with the excitation of other nonlinear oscillators, taking advantage of the common structure of different self-sustained oscillators, first discovered in (McIntyre et al., 1983).

In this way we are able to obtain waveforms which, starting from the well-known Helmholtz motion, i.e., the ideal motion of a bowed string, move toward motions which are characteristics of other self-sustained oscillators.

This was done in order to extend the bowed string to a more general oscillators more interesting from a compositional point of view.

3.5 Controlling the physical model

In order to play the physical model in real-time we experimented with various controllers. The main problem we encountered was to be able to find a controller that was both playable and able to explore the large combinations of parameters that the model was able to create. We were also interested on creating a virtual instrument with a different gestural control than the real bowed strings.

We therefore decided to experiment with an alternate controller, the metasaxophone, as described in the following section.

3.6 The metasaxophone

In an effort to explore extended techniques of the bowed string physical model we perform it with an original alternate controller, the metasaxophone (Burtner, 2002), shown below. The development of the Metasaxophone drew on a growing body of important alternate controller work (Scavone, 1999; Cook, 1992). The instrument itself was named specifically in reference to Cook's work with wind instrument physical models and alternate controllers (Cook, 1992).

The metasaxophone is an acoustic Selmer tenor saxophone retrofitted with sensors and a microprocessor that converts performance data into MIDI control messages. The microprocessor gathers performance data from eight continuous controller force sensing resistors (FSR), five triggers, and an accelerometer. The Interlink Electronics FSRs are located on the front B, A, G, F, E and D keys, and beside each of the thumb rests. Three triggers (also Interlink Electronic FSRs used as triggers) are located on the bell of the instrument, and one below each of the thumb rests. An Analog Devices ADXL202 accelerometer IC chip on the bell measures the position of the saxophone on a two dimensional axis – left/right and up/down.

The data from these sensors are collected via a 26 pin serial connector by a Basic Stamp BIISX microprocessor fixed to the bell of the instrument. Analog pressure data from the performer is converted to a digital representation by passing each analog signal through a resistor/capacitor (RC)



Fig. 6. The metasaxophone: front and back views.

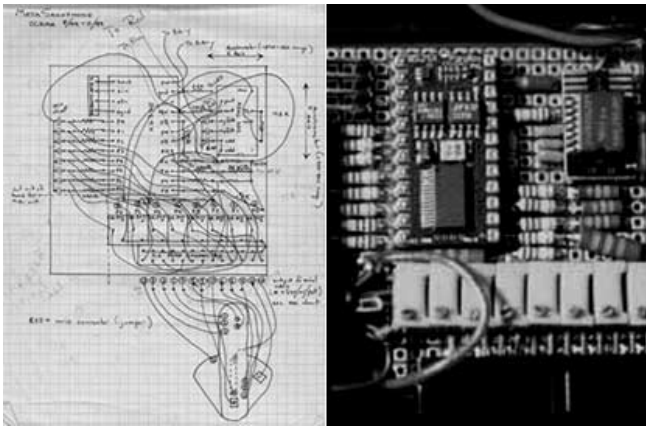


Fig. 7. Metasaxophone Circuit Diagram and Corresponding Circuit Board.

circuit into the input pins on the BIISX. Trim potentiometers calibrate the sensitivity of each sensor. Figure 7 illustrates the metasaxophone circuit block diagram.

The BIISX is programmed in Parallax Basic (PBASIC) and the software converts the sensor data into MIDI messages. Analog to digital conversion is accomplished using the PBASIC *RCTIME* (Parallax inc, 1999) function which measures the charge/discharge time of the RC circuit over time. The metasax program loops through the input pins reading the *RCTIME* counter of each pin.

Multiple programs can be loaded into the BIISX's EEPROM for a variety of applications. The standard metasaxophone software sends MIDI control change messages 20–27 for the FSRs, MIDI note-on 1–5 for the triggers, and the accelerometer sends MIDI note-on messages 6–10 as the performer crosses certain thresholds of left/right, up/down tilt.

The circuit board and a 9-volt battery are fit into a plastic box with openings cut for the serial cable inputs, the MIDI

output connector, a power switch, and a power light. MIDI messages from the metasaxophone can be sent to any MIDI device and used as control data for live electronics.

In addition to sending MIDI information, the metasaxophone sends an audio signal through small microphones located inside and around the bell. The microphone system was also created especially for the metasaxophone and consists of small Panasonic condenser electret cartridges fitted to the ends of bendable tubing and wrapped with the microphone wires inside heat-shrink tubing. The microphone system is designed to attach to the back of the metasaxophone circuit box on the top of the bell, and each mic can be placed independently at the desired location around or inside the instrument. In the standard configuration, one mic is positioned deep inside the bell, without touching the inner walls of the instrument. The circuit of this mic was modified to handle higher sound pressure levels without distortion. Two other mics are positioned outside the horn, one on the lower half and the other on the upper half/neck area. This configuration allows for close mic'ing of the instruments' low resonances, high frequencies, and mid-range frequencies. The mics, however, can be placed in any configuration depending on the application needed, and each has a separate output allowing the signals to be routed to separate devices for processing or to multiple channels on a mixer.

The continuous controller MIDI messages sent from the metasaxophone are used to control digital signal processing and synthesis algorithms. Similarly, the audio is used as a control signal to alter the function of the MIDI data or to control other sonic parameters. Both MIDI and audio data are sent to some external computer or device for processing. Currently we are using an interface created in Max/MSP (Zicarelli, 1998).

4. Instrument controller substitution

The timbral space of the ExBow bowed string physical model is controlled by the metasaxophone, the key pressures applied to the metasaxophone's keys acting as individual input controls for the model. By assigning each key of the saxophone to a different parameter of the model, the bowing action is broken into a series of isolated tasks. This creates a reallocation of the parameters of a complex expressive action – the bowing – to another complex action – the fingering of keys. Consequently simple motions such as the convergence of parameters occurring when, for example, a bow is drawn across the strings can become difficult to execute, while impossible bowing actions, such as rapidly fluctuating the bow position while applying extreme bow pressure, become possible.

The extended bowed string physical model is an external extension to the Max/MSP program called ExBow~. The input parameters of the physical model, i.e., bow pressure, bow velocity, bow position, string inharmonicity, frictional

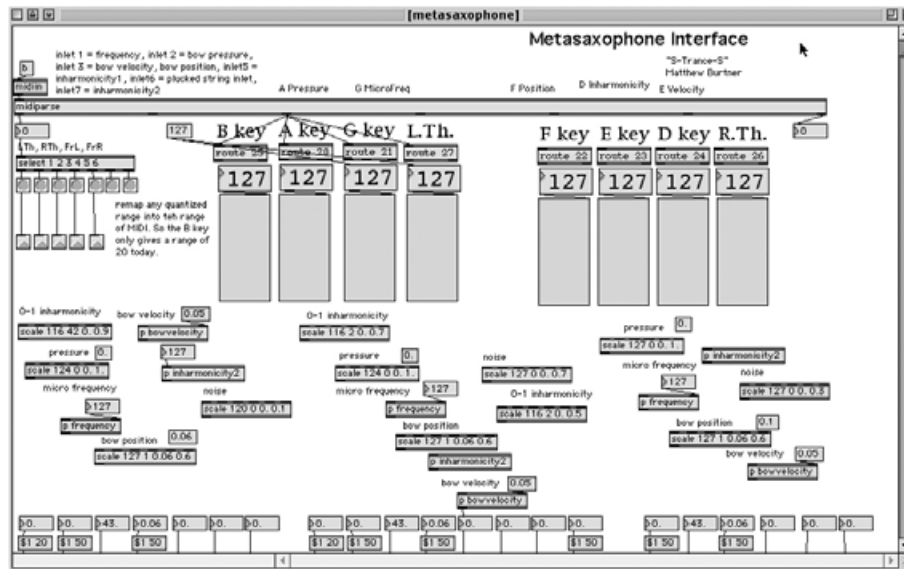


Fig. 8. Max/MSP patch mapping the metasax to the inputs of the bowed string model.

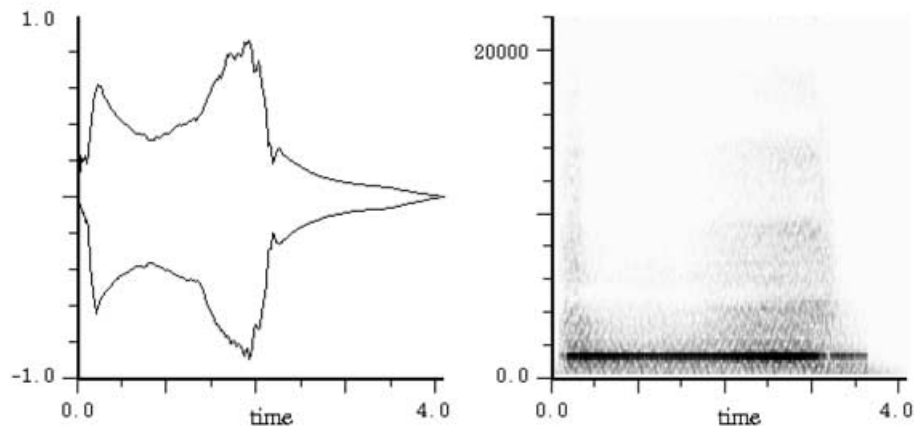


Fig. 9. Variation of bow pressure and velocity. Right: time domain representation, left: sonogram.

properties, center frequency, and microtonal frequency variation are controlled by different sensors on the metasaxophone, as shown in Figure 8.

By allowing the physical model to be controlled from within the gestural space of a wind instrument, new expressive potentialities of the model are opened. A series of expression tests of this nature were performed. These tests suggested new possibilities of exploring extended techniques for physical models using instrument controller substitution remappings. Furthermore, the acoustics of these results suggested additional extensions to the acoustic properties of the string physical model itself. The following section illustrates ways in which this process is applied by the metasaxophone controller.

5. Instrument controller substitution and sound examples

- In the first example (Fig. 9), the stroke starts with extreme bow pressure but no bow velocity. The bow is then moved quickly across the string and simultaneously the pressure is dropped. The pressure is then increased again and cut off abruptly. During this action, the overtones can be controlled by the degree and cut-off rate of the bow pressure.
- The second example (Fig. 10) illustrates a situation that would be impossible on a violin controller but that is idiomatic for the metasaxophone controller. Extreme pressure is applied to the string and a very slow velocity is maintained. But simultaneously, the bow position changes

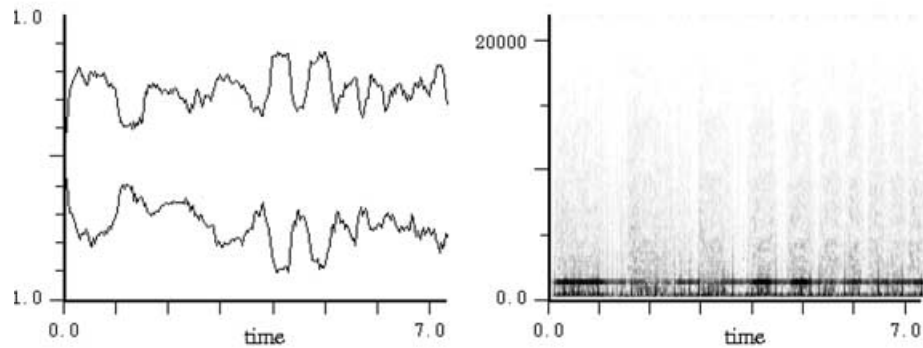


Fig. 10. Fast movements from the bridge to the nut. Right: time domain representation, left: sonogram.

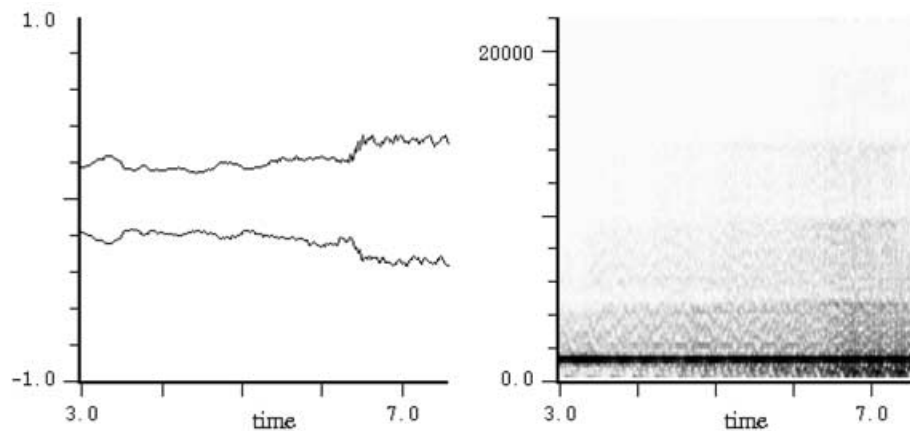


Fig. 11. Variation of the inharmonicity of the string. Right: time domain representation, left: sonogram.

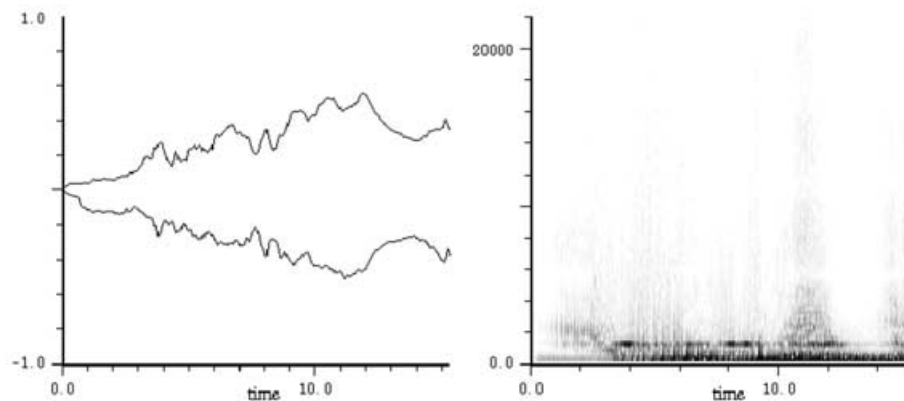


Fig. 12. Transformations of different parameters of the string. Right: time domain representation, left: sonogram.

rapidly from a location very near the bridge to a location high on the fingerboard. The rate of oscillation is accelerated steadily.

- The third example (Fig. 11) reveals an attempt to isolate the inharmonicity parameter of the string by attempting a regular bowing action while simultaneously changing finger pressure on the D key of the saxophone. The result approximates a case in which the string is transformed from nylon into glass during the bowing. The normal

change of inharmonicity causes a drop in frequency, and this tendency is compensated for in the example by raising the micro-frequency of the pitch.

- The fourth example (Fig. 12) utilizes transformations of inharmonicity, bow pressure, bow speed, frequency, and micro-frequency. In this example, the complex changes in all parameters are combined in order to present a rich and expressive musical gesture. The example illustrates that extended techniques for physical models can arise natu-

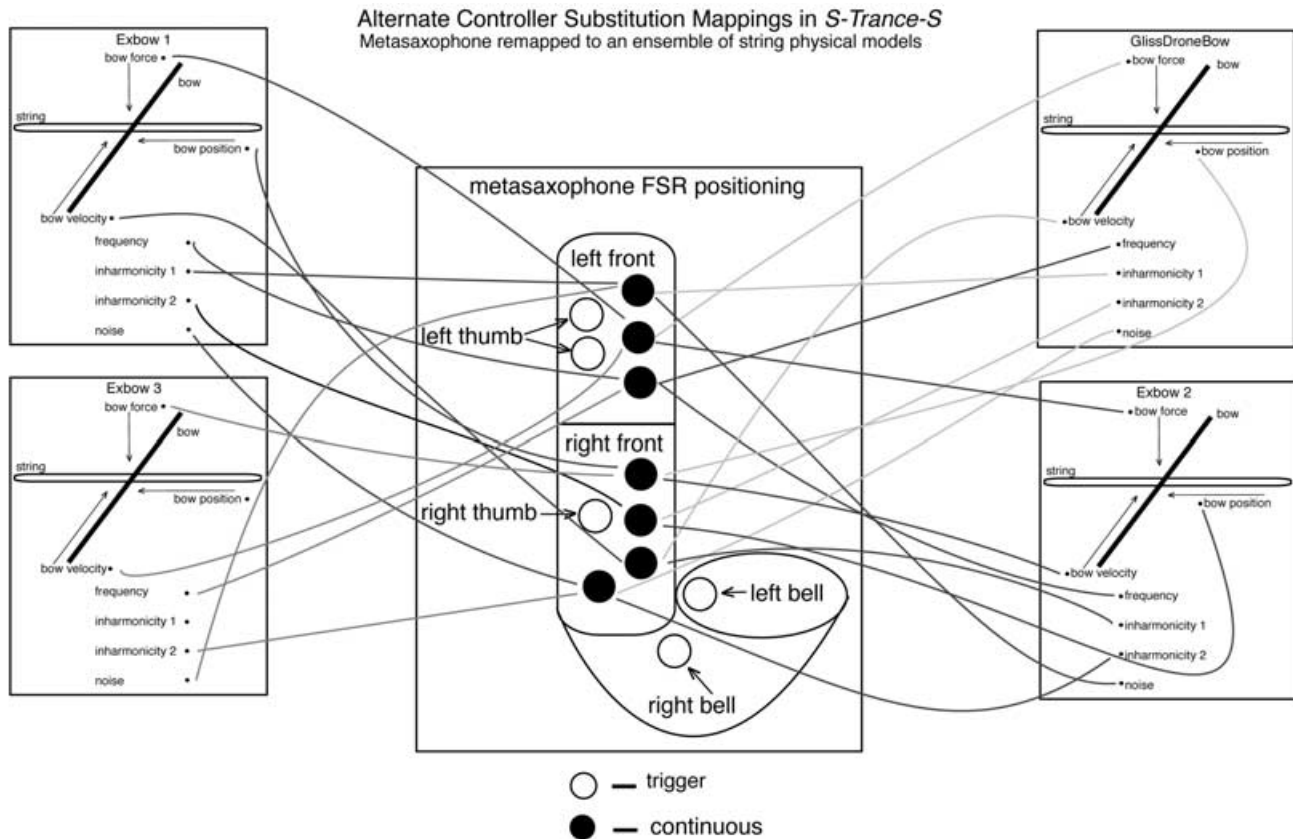


Fig. 13. Metasax/ExBow Controller Mappings in *S-Trance-S*.

rally from the remapping of performance data from one controller action to another.

6. Composition: *S-Trance-S*

In the musical composition, *S-Trance-S* (2001), written expressly for this instrumental configuration, we explore instrument controller substitution through the metamorphosis between “real” and physically modelled instruments. The metasaxophone keys are mapped to the physical model bowing parameters: bow force, bow position, bow velocity, frequency, two types of inharmonicity, and chaotic bow friction. Figure 13 illustrates the mappings as they occur in the piece.

This controller mapping then undergoes a series of remappings as the single virtual string grows into an ensemble of virtual strings, each one utilizing a different controller mapping. With regard to the physical model it was compositionally relevant to identify two types of control parameters, (1) those that are intrinsically tied to the generation of sound such as bow velocity and bow pressure, and (2) those that modify the mode of performance for expressive timbral richness such as inharmonicity, noise, bow position, and frequency. This observation was an important concern when creating the performance mappings

because for a generally congruous sound certain keys must retain a propagatory role while others can be used as modifiers.

The metasaxophone controls the transformation between three instruments: the acoustic saxophone, a string physical model played by the metasaxophone controllers, and acoustic bowed string timbres played by the computer. Two aspects of extended techniques for physical models are explored – gestural transmutation of the instrumental controller, and signal transmutation as a result of instrumental cross synthesis.

Through signal transmutation, the saxophone sound, the bowed string sound, and the combined metasax/string physical model sound are transformed into a series of hybrid instruments that are performed live by the saxophone and transfused into independent timbral screens. There are six such convolved timbral screens derived from the three archetypal models

- 1) Sax convolved with sax
- 2) String convolved with string
- 3) Physical model string convolved with physical model string
- 4) Sax convolved with physical model string
- 5) Sax convolved with string
- 6) Physical model string convolved with string

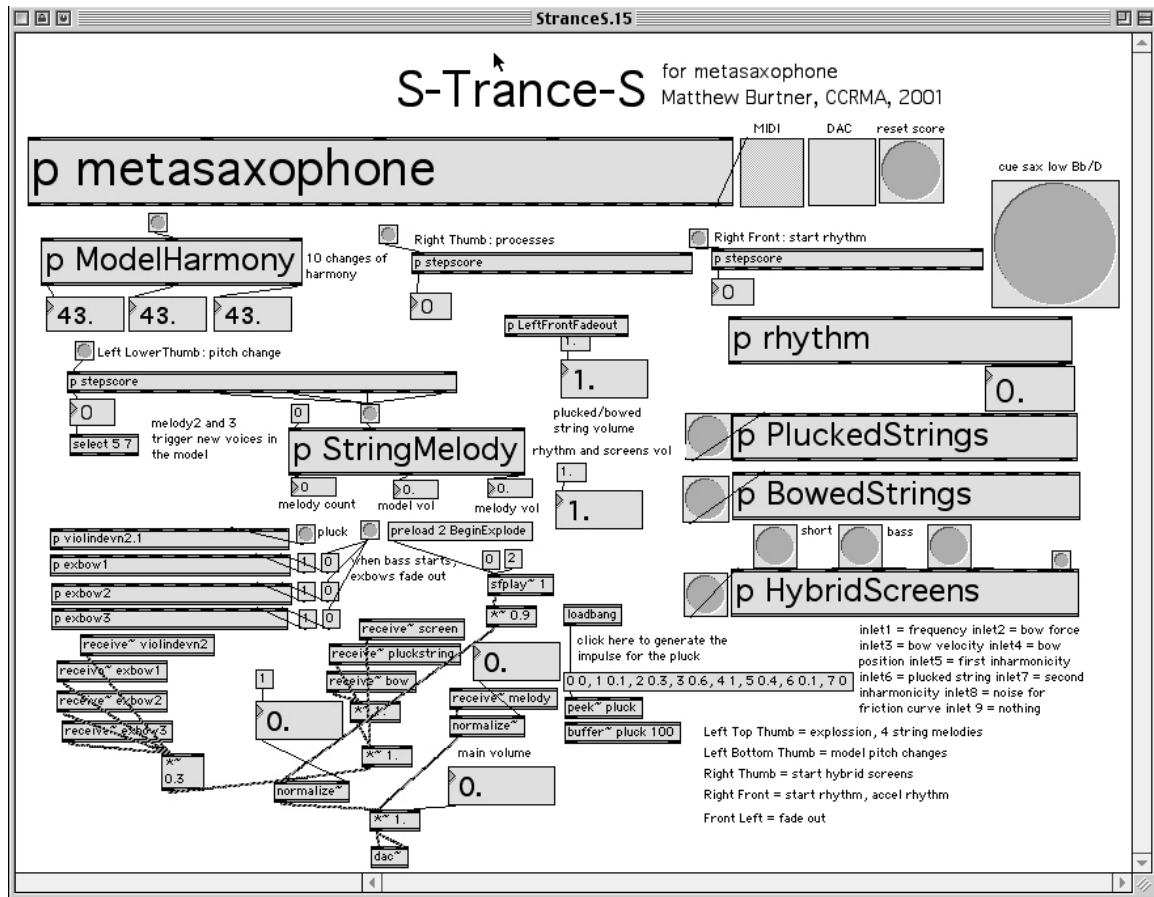


Fig. 14. *S-Trance-S* performance interface.

As these hybrid timbres evolve they are continuously mutated, forming a series of transformations. Figure 14 shows the Max/MSP interactive performance interface for *S-Trance-S*. The metasaxophone ExBow interface (Fig. 8) is located inside the “metasaxophone” subpatch.

S-Trance-S was premiered at Mills College in Oakland on February 16, 2001.

7. Conclusion

Instrumental controller substitution opens new paradigms for compositional timbral exploration using physical models. Rather than evaluating the musical effectiveness of the physical model in terms of its acoustic real-world counterpart, the virtual instrument is explored for its own complex and unique properties. Similarly, the instrumental controller when coupled with the physical model can be evaluated independently from its acoustic basis, solely as a controller for the redefined digital instrument. “*S-Trance-S*” explores this paradigm of transmutation by seeking to occupy a new timbrally rich musical space in which a dialectic is established between control parameters and sonic parameters. This type of coupling is natural with all musical instruments but instrumental controller substitution opens the

possibility of potentially unlimited hybrid electroacoustic instruments.

References

- Burtner, M. (2002). “The Metasaxophone: Concept, Implementation, and Mapping Strategies for a New Computer Music Instrument,” *Organized Sound*, vol. 7, n.2.
- Cook, P. (1992). “A Meta-Wind-Instrument Physical Model, and a Meta-Controller for Real Time Performance Control,” International Computer Music Conference, San Jose, Oct.
- Cremer, L. (1984). “The Physics of the Violin,” MIT Press, Cambridge, MA.
- Fletcher, N.H. & Rossing, T.D. (1998). “The Physics of Musical Instruments,” Second Edition, Springer Verlag, New York.
- Lang, M. (1992). “Optimal Weighted Phase Equalization According to the 1-infinity norm,” *Signal Processing*, vol. 27, pp. 87–98.
- McIntyre, M.E., Schumacher, R.T., & Woodhouse, J. (1981). “Aperiodicity in Bowed-String Motion,” *Acustica*, vol. 49, n.1, pp. 13–32.
- McIntyre, M.E., Schumacher, R.T., & Woodhouse, J. (1985). “On the oscillations of musical instruments,” *JASA*, vol. 74, n.5, pp. 1325–1345.

- Morse, P.H. (1981). "Vibration and Sound," *American Institute of Physics for the Acoustical Society of America*, 4th edition.
- Parallax Incorporated (1999). "BASIC Stamp Programming Manual," Version 1.0. <http://www.parallaxinc.com>.
- Rocchesso, D. & Scalcon, F. (1996). "Accurate Dispersion Simulation For Piano Strings," *Nordic Acoustical Meeting*, Helsinki.
- Salisbury, J.K., Townsend, W.T., Eberman, B.S., & DiPietro, D.M. (1988). "Preliminary Design of a Whole-Arm Manipulation System (WAMS)," Proc. Of the 1988 Int. Conf. On Robotics and Automation, Philadelphia, Pa: IEEE, pp. 254–60.
- Scavone, Gary. (1999). "The Holey Controller". At <http://www-ccrma.stanford.edu/~gary>.
- Serafin, S., Smith J.O. III, & Woodhouse, J. (1999). "An Investigation of the Impact of Torsion Waves and Friction Characteristics on the Playability of Virtual Bowed Strings," IEEE Workshop on Applications of Signal Processing to Audio and Acoustics, *IEEE Press*, New York.
- Smith, J.H. & Woodhouse, J. (2000). "The Tribology of Rosin." *J. Mech. Phys. Solids*, vol. 48, pp. 1633–1681.
- Smith, J.O. III (1983). "Techniques for Digital Filter Design and System Identification with Application to the Violin," *PhD thesis*, Stanford University.
- Smith, J.O. III & Abel, J.S. (1999). "Bark and ERB Bilinear Transforms," *IEEE Trans. Speech and Audio Processing*.
- Woodhouse, J. & Loach A.R. (1999). "The Torsional Behavior of Cello Strings," *Acustica – ACTA Acustica*, vol. 85.
- Zicarelli, D. (1998). *An Extensible Real-Time Signal Processing Environment for Max*, Proceedings of the International Computer Music Conference, Ann Arbor, Michigan.